ACCESS CellPress
Cell Reports
Report

Uterine Leiomyoma-Linked MED12 Mutations Disrupt Mediator-Associated CDK Activity

Mikko Turunen,[1,8] Jason M. Spaeth,[2,8] Salla Keskitalo,[3] Min Ju Park,[2] Teemu Kivioja,[1,4] Alison D. Clark,[2] Netta Mäkinen,[5] Fangjian Gao,[2] Kimmo Palin,[1] Helka Nurkkala,[3] Anna Vähärautio,[1,6] Mervi Aavikko,[5] Kati Kämpjärvi,[5] Pia Vahteristo,[5] Chongwoo A. Kim,[7] Lauri A. Aaltonen,[5] Markku Varjosalo,[3,*] Jussi Taipale,[1,6,*] and Thomas G. Boyer[2,*]

[1]Genome-Scale Biology Program and Department of Pathology, Haartman Institute, University of Helsinki, Biomedicum, P.O. Box 63 (Haartmaninkatu 8), Helsinki FIN-00014, Finland
[2]Department of Molecular Medicine, Institute of Biotechnology, University of Texas Health Science Center at San Antonio, 7703 Floyd Curl Drive, Mail Code 8257, STRF, San Antonio, TX 78229-3900, USA
[3]Institute of Biotechnology, University of Helsinki, Viikinkaari 1, P.O. Box 65, Helsinki FIN-00014, Finland
[4]Department of Computer Science, University of Helsinki, P.O. Box 68, Helsinki FIN-00014, Finland
[5]Genome-Scale Biology Program and Department of Medical Genetics, Haartman Institute, University of Helsinki, Biomedicum, P.O. Box 63 (Haartmaninkatu 8), Helsinki FIN-00014, Finland
[6]Science for Life Laboratory, Department of Biosciences and Nutrition, Karolinska Institutet, Stockholm 14183, Sweden
[7]Department of Biochemistry, University of Texas Health Science Center at San Antonio, 7703 Floyd Curl Drive, San Antonio, TX 78229-3900, USA
[8]Co-first author
*Correspondence: markku.varjosalo@helsinki.fi (M.V.), jussi.taipale@ki.se (J.T.), boyer@uthscsa.edu (T.G.B.)
http://dx.doi.org/10.1016/j.celrep.2014.03.047

SUMMARY

Somatic mutations in exon 2 of the RNA polymerase II transcriptional Mediator subunit *MED12* occur at very high frequency (~70%) in uterine leiomyomas. However, the influence of these mutations on Mediator function and the molecular basis for their tumorigenic potential remain unknown. To clarify the impact of these mutations, we used affinity-purification mass spectrometry to establish the global protein-protein interaction profiles for both wild-type and mutant MED12. We found that uterine leiomyoma-linked mutations in MED12 led to a highly specific decrease in its association with Cyclin C-CDK8/CDK19 and loss of Mediator-associated CDK activity. Mechanistically, this occurs through disruption of a MED12-Cyclin C binding interface that we also show is required for MED12-mediated stimulation of Cyclin C-dependent CDK8 kinase activity. These findings indicate that uterine leiomyoma-linked mutations in MED12 uncouple Cyclin C-CDK8/19 from core Mediator and further identify the MED12/Cyclin C interface as a prospective therapeutic target in CDK8-driven cancers.

INTRODUCTION

Uterine leiomyomas (fibroids) are monoclonal neoplasms of the myometrium and represent the most common pelvic tumor in reproductive-age women (Stewart, 2001). Although benign, they are nonetheless associated with significant morbidity. They are the primary indicator for hysterectomy and a major cause of gynecologic and reproductive dysfunction, ranging from profuse menstrual bleeding and pelvic discomfort to infertility, recurrent miscarriage, and preterm labor (Stewart, 2001). Recently, we discovered that mutations in exon 2 of the *Xq13* gene encoding the transcriptional Mediator subunit *MED12* occur at very high frequency (~70%) in uterine leiomyomas (Mäkinen et al., 2011). Along with their high-frequency occurrence, two additional genetic findings suggest that MED12 mutations likely contribute to the genesis of uterine leiomyomas. First, all observed MED12 exon 2 mutations affect highly evolutionarily conserved regions of the MED12 protein, including three principal hot spot mutations in codons 36, 43, and 44 (Mäkinen et al., 2011). Second, localization of the missense mutations to a small number of amino acids suggests that the MED12 mutations are dominant and that MED12 acts as an oncogene (Vogelstein et al., 2013), providing a likely etiological basis previously lacking for the majority of these clinically significant tumors. Compatible with the key role of MED12 in controlling gene expression, we have also shown that the RNA expression patterns of MED12 mutant leiomyomas cluster tightly together and form a clearly separate branch distinct from all other leiomyomas (Mehine et al., 2013).

Mediator is a conserved multisubunit signal processor through which regulatory information conveyed by gene-specific transcription factors is transduced to RNA polymerase II (pol II). Structurally, Mediator is assembled from a set of core subunits into three distinct modules, termed "head," "middle," and "tail," that bind tightly to pol II in the so-called holoenzyme (Conaway and Conaway, 2011; Kornberg, 2005; Larivière et al., 2012; Malik and Roeder, 2010; Spaeth et al., 2011; Taatjes, 2010). MED12, along with MED13, Cyclin C, and CDK8 or CDK19, comprise a fourth "kinase" module that exists in variable association with core Mediator. The kinase module was originally implicated in negative regulation of pol II-dependent transcription

(Akoulitchev et al., 2000; Knuesel et al., 2009a; van de Peppel et al., 2005). Several more recent studies, however, have also characterized a positive role for CDK8 activity in transcription (Donner et al., 2010; Firestein et al., 2008; Morris et al., 2008).

MED12 links Cyclin C-CDK8 with core Mediator and also stimulates Cyclin C-dependent CDK8 kinase activity (Ding et al., 2008; Knuesel et al., 2009b). Although the mechanism by which MED12 activates CDK8 is unknown, MED12-dependent CDK8 activation is nonetheless required for nuclear transduction of signals propagated by several different oncogenic pathways with which MED12 is biochemically and genetically linked (Firestein et al., 2008; Kim et al., 2006; Spaeth et al., 2011; Zhou et al., 2006, 2012). Furthermore, MED12 itself is a target of oncogenic mutation, including exon 2 mutations linked to uterine leiomyomas (Barbieri et al., 2012; Je et al., 2012; Kämpjärvi et al., 2012; Mäkinen et al., 2011). However, the impact of these mutations on MED12 function and the molecular basis for their tumorigenic potential remain unknown.

RESULTS AND DISCUSSION

Uterine Leiomyoma-Linked Mutations in MED12 Disrupt its Association with Cyclin C-CDK8/CDK19

To identify proteins that bind differentially to wild-type (WT) and oncogenic MED12, we engineered stable, tetracycline-inducible Flp-In 293 T-REx cell lines expressing C-terminally Twin-Strep-tag-modified WT MED12 or its most common leiomyoma mutant derivative (G44D) (see Experimental Procedures for details) (Glatter et al., 2009; Varjosalo et al., 2013). Quantitative immunoblot analysis revealed that tagged WT and mutant MED12 proteins attained induced levels of expression (~0.8–1.6 × 10^5 molecules per cell) comparable to that of endogenous 293 cell MED12 (~0.4–0.8 × 10^5 molecules per cell) (Figure S1A). Affinity-purification mass spectrometry (MS) (Figure 1A; Figure S1B) revealed a specific and reproducible (n = 3) reduction in the binding of Cyclin C, CDK8, and CDK19 to mutant versus WT MED12 (Figure 1B; Table S1).

Relative quantification of MED12-associated Mediator subunits confirmed a statistically significant loss of kinase module, as opposed to core Mediator subunits, in mutant versus WT MED12 affinity purifications (Figure 1C; Table S2). We confirmed the reduced association of CDK8 and CDK19 with MED12 G44D by immunoprecipitation (IP)-western blot (Figure 1D) and further established that this defect extends to other uterine leiomyoma-linked exon 2 mutations in MED12, including L36R, Q43P, and G44S. Thus, FLAG-specific immunoprecipitates from HEK293 cells expressing FLAG-tagged MED12 mutant derivatives bore significantly reduced levels of Cyclin C, CDK8, and CDK19, but not core Mediator subunits, as well as diminished pol II C-terminal domain (CTD)-directed kinase activity compared to those from WT MED12-expressing cells (Figure 1E).

Uterine Leiomyoma-Linked Mutations in MED12 Disrupt Its Direct Interaction with Cyclin C-CDK8

To determine whether leiomyoma-linked mutations in MED12 disrupt its direct interaction with Cyclin C-CDK8, we analyzed recombinant kinase module variants reconstituted from baculovirus-expressed subunits. CDK8 immunoprecipitates from insect cells coexpressing CDK8, Cyclin C, and either WT or mutant MED12 derivatives (L36R, Q43P, or G44S) were monitored for the presence of MED12 and the level of CDK8 kinase activity. Note that these reconstitution assays were performed in the absence of MED13, because the latter does not appreciably impact the integrity or activity of a trimeric MED12/Cyclin C/CDK8 submodule assembly (Figure S1C). Compared to WT MED12, all three of the MED12 leiomyoma mutants were severely compromised for both Cyclin C-CDK8 binding and activation (Figure 1F). We mapped the Cyclin C-CDK8 binding domain on MED12 to within its N-terminal 100 amino acids encoded largely by exons 1 and 2 (Figures 2A and 2B) and further confirmed that MED12 (1–100) binds to and activates Cyclin C-CDK8 (Figure 2C). This suggests that exon 2 mutations in MED12 likely disrupt its Cyclin C-CDK8 binding interface as opposed to triggering conformational masking of a distant interaction site elsewhere in the protein. Together, these findings identify a common functional defect associated with uterine leiomyoma-linked mutations in MED12 and further suggest that disruption of its Cyclin C-CDK binding activity contributes to leiomyoma formation.

MED12 Activates CDK8 through Direct Interaction with Cyclin C

To clarify the molecular basis by which exon 2 mutations in MED12 disrupt its direct interaction with Cyclin C-CDK8, we first resolved kinase module subunit interactions using recombinant baculovirus-expressed proteins. Immunopurification of the kinase module from insect cells expressing all possible combinations of its four constituent subunits permitted resolution of its hierarchical subunit organization. This analysis revealed that MED12 binds to Cyclin C, which in turn binds to CDK8 (Figure 3A; Figure S2A). MED12 also binds to MED13, which does not bind to either Cyclin C or CDK8 (Figure 3A; Figures S2A and S2B). Importantly, we did not detect an interaction between MED12 and CDK8 in the absence of Cyclin C (Figure 3A; Figures S2A and S2C), indicating that Cyclin C bridges MED12 and CDK8. These findings confirm those recently described for subunit assembly in *S. cerevisiae* and support a conserved molecular organization between the yeast and human kinase modules (Tsai et al., 2013).

To understand how MED12 binds to Cyclin C, we exploited information derived from prior structural resolution of both *S. pombe* and *H. sapiens* Cyclin C proteins (Hoeppner et al., 2005; Schneider et al., 2011). These structures reveal the presence of a unique surface groove that is phylogenetically conserved among Cyclin C family members but absent from cell-cycle-type cyclins (Figure 3B). We hypothesized that this surface groove could represent a binding interface through which MED12 stimulates Cyclin C-dependent CDK8 kinase activity. To test this hypothesis, we introduced substitution mutations at residues both within (W177A, N181A, D182A, and Y238A) and outside of (W6A and E98A) the structurally defined Cyclin C surface groove (Figure 3B) and examined their impact on MED12 binding and CDK8 activation. Accordingly, CDK8-specific immunoprecipitates from insect cells coexpressing CDK8, MED12, and either WT or mutant Cyclin C derivatives were examined for both the presence of MED12 and the

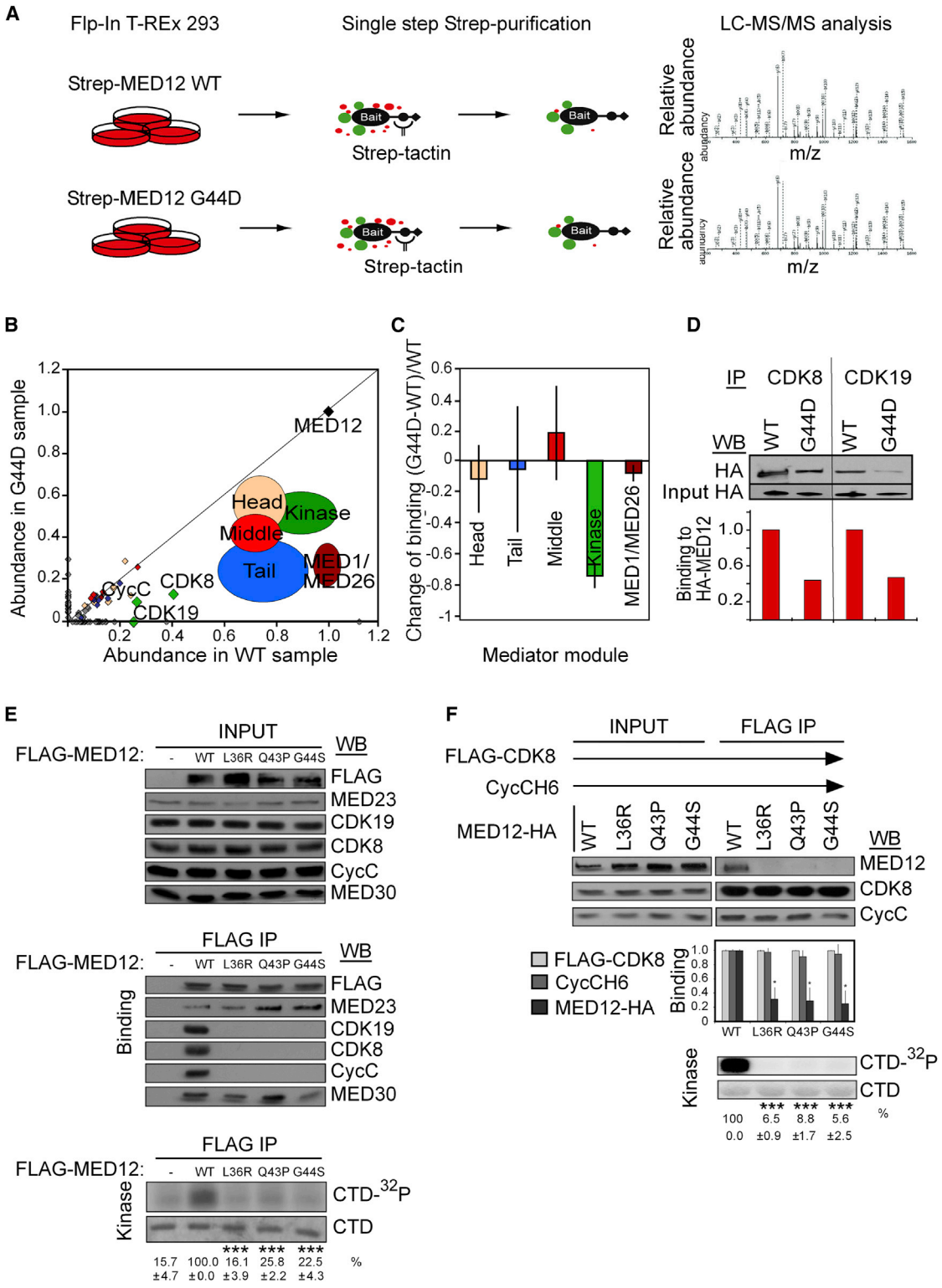

Figure 1. Leiomyoma-Linked Mutations in MED12 Disrupt its Interaction with Cyclin C-CDK8/19 and Diminish Mediator-Associated Kinase Activity

(A) Schematic illustration of MED12 WT and G44D mutant protein-protein-interactome screen.

(B) Normalized abundance of MED12 WT and G44D-interaction proteins. Modular arrangement of the Mediator is shown. Note that MED12 mutation G44D results in specific decrease in binding of kinase module subunits.

(legend continued on next page)

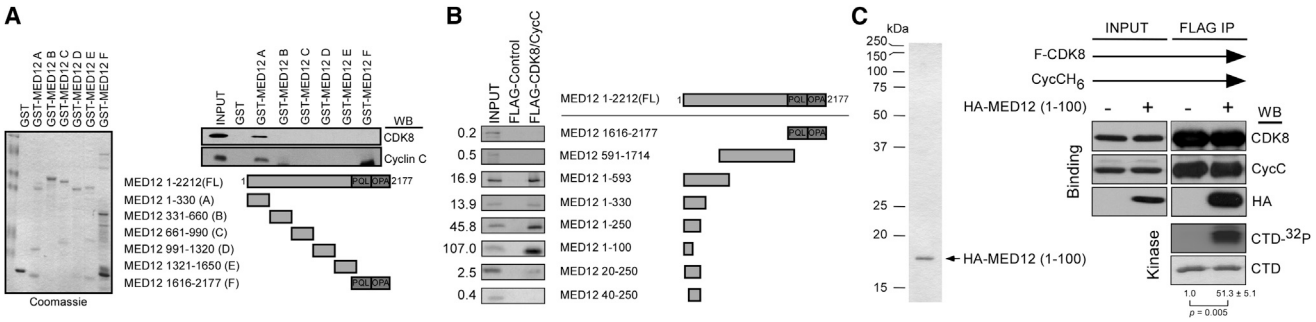

Figure 2. The MED12 N-Terminal 100 Amino Acids Bind to and Activates Cyclin C-CDK8

(A) Glutathione S-transferase (GST)-MED12 fragments as indicated were immobilized on glutathione-Sepharose and incubated with insect cell lysates coexpressing Cyclin C/CDK8. Bound proteins were eluted with Laemmli sample buffer and resolved by SDS-10% PAGE prior to visualization by Coomassie blue staining (left) or WB analysis (right) using antibodies specific for CDK8 and Cyclin C. INPUT, 10% of insect cell lysate used in GST pull-down reactions.

(B) FLAG-specific immunoprecipitates from insect cells infected without (FLAG-Control) or with (FLAG-CDK8/CycC) baculoviruses expressing FLAG-CDK8 and CycCH6 were incubated with the indicated ^{35}S-labeled MED12 truncation fragments produced by transcription and translation in vitro. Bound proteins were eluted with Laemmli sample buffer and resolved by SDS-12% PAGE prior to visualization by Phosphorimager analysis. INPUT, 10% of the in vitro translated MED12 protein fragments used in binding reactions. Phosphorimager signals were quantified, and the level of binding for each MED12 fragment to CDK8/Cyclin C is expressed relative to the 10% INPUT signal.

(C) (Left) Purified HA-MED12 (1–100) bearing tandem six-histidine and hemagglutinin (HA)-epitope tags was expressed in *E. coli* and purified on nickel-nitrilotriacetic acid prior to resolution by SDS-15% PAGE and visualization by Coomassie blue staining. Molecular weight marker positions (kDa) are indicated. (Right) Baculovirus-expressed Cyclin C-H6/FLAG-CDK8 was immunoprecipitated from infected insect cell lysates in the absence (–) or presence (+) of HA-MED12 (1–100). FLAG-specific immunoprecipitates were processed by western blot using the indicated antibodies (top) or incubated with [γ-^{32}P]-ATP and purified GST-CTD (bottom). INPUT corresponds to 5% of protein used in IP reactions. ^{32}P-GST-CTD levels were quantified and expressed relative to the level in the absence of MED12 (1–100). Data represent the average ± SEM of three independent experiments. p value calculated by Student's t test.

level of CDK8 kinase activity. Three surface-groove mutants (N181A, D182A, and Y238A), but no mutant outside the groove, diminished MED12 binding and CDK8 kinase activity (Figure 3C) without affecting CDK8 binding. These results identify the Cyclin C surface groove as a principal binding interface through which MED12 activates CDK8 and further reveal that MED12 and CDK8 bind to Cyclin C through distinct surfaces.

To confirm these findings in vivo, we expressed FLAG-tagged WT Cyclin C or its MED12 binding-deficient mutant derivative (N181A) in HEK293 cells and monitored their chromatographic elution profiles by gel filtration analysis. Whereas WT Cyclin C coeluted along with other Mediator subunits in a ~2 MDa Mediator peak, Cyclin C N181A was excluded entirely from these fractions (Figures S3A and S3B), indicating that surface-groove mutations disrupt the association of Cyclin C with MED12, its principal anchor in Mediator. This interpretation is congruent with coimmunoprecipitation analyses from FLAG-tagged WT and mutant Cyclin C-expressing cells. FLAG-specific immunoprecipitates from N181A and D182A-expressing cells harbored CDK8, but not MED12 or other Mediator subunits that were readily detected in those from WT and E98A-expressing cells (Figure 3D). Concordantly, Cyclin C-associated CDK8 kinase activity was significantly reduced in FLAG-specific immunoprecipitates from cells expressing N181A and D182A compared to WT or E98A derivatives (Figure 3D). Together, these results identify the Cyclin C surface groove as a principal binding interface through which MED12 both anchors Cyclin C-CDK8 into Mediator and stimulates Cyclin C-dependent CDK8 kinase activity.

(C) Average change of binding of MED12 G44D mutant to different Mediator modules. Data represent the average ± SD of three independent experiments. The only statistically significant change was found with the kinase module ($p = 2 \times 10^{-5}$). For the other modules, $p > 0.2$. See Table S2 for description of statistical analysis.

(D) Immunoprecipitation (IP)-western blot (WB) verification of the loss of CDK8/CDK19 binding to the G44D mutant MED12 from 293 Flp-In cells.

(E) FLAG-tagged WT MED12 or its indicated mutant derivatives were immunoprecipitated from transfected HEK293 cell lysates. FLAG-specific immunoprecipitates were processed by WB using the indicated antibodies (middle panel) or incubated with [γ-^{32}P]-ATP and purified glutathione S-transferase (GST)-CTD (bottom). INPUT (top) corresponds to 10% of cell lysate used in IP reactions. ^{32}P-GST-CTD levels were quantified and expressed relative to the level in the WT MED12 IP. Data represent the average ± SEM of three independent experiments. Asterisks denote statistically significant differences versus WT (Student's t test, ***$p < 0.001$). Note that the CDK19 WB was derived from the same IP but a different gel to preclude interference from the signal produced by similarly sized CDK8.

(F) Baculovirus-expressed FLAG-CDK8, Cyclin C-H6, and MED12-HA (WT or mutant as indicated) were immunoprecipitated from infected insect cell lysates. FLAG-specific immunoprecipitates were processed by WB using the indicated antibodies (top) or subjected to in vitro kinase assay (bottom) as in (E). Input corresponds to 10% of cell lysate used in IP reactions. WBs were quantified and levels of MED12 and Cyclin C (CycC) in each IP were normalized to CDK8 levels and expressed relative to their corresponding normalized levels in the CDK8/CycC/MED12 WT IP (middle). ^{32}P-GST-CTD levels in each IP/kinase reaction were quantified and expressed relative to the level in the CDK8/CycC/MED12 WT IP. Data represent the average ± SEM of three independent experiments. Asterisks denote statistically significant differences versus WT (Student's t test, *$p < 0.05$, ***$p < 0.001$).

See also Figure S1 and Tables S1–S3.

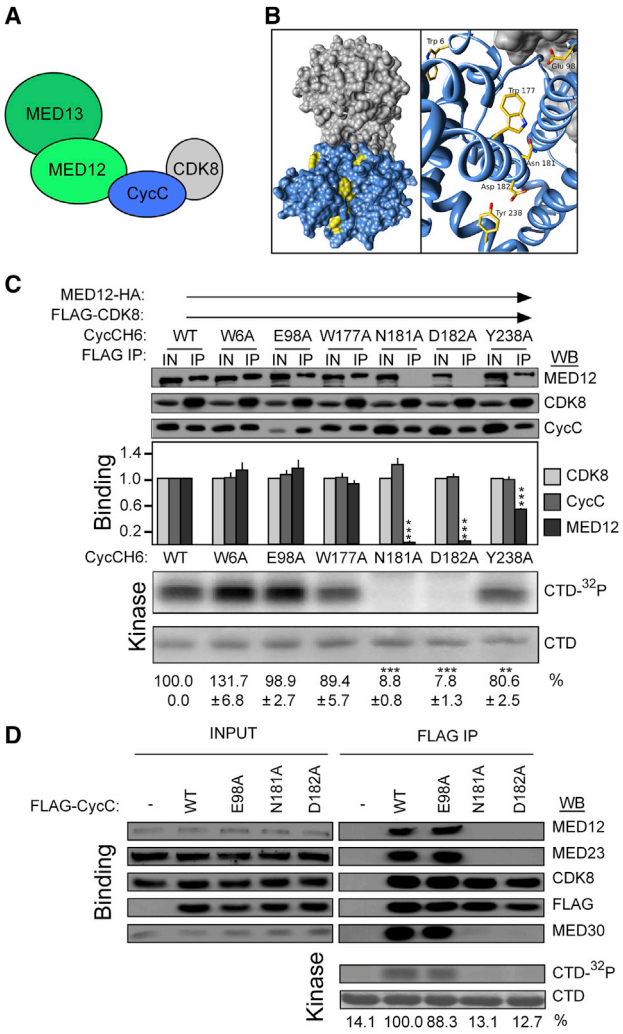

Figure 3. The Cyclin C Surface Groove Is Required for MED12 Binding and CDK8 Activation

(A) Schematic summary of binding interactions within the Mediator kinase module.

(B) Structure of *H. sapiens* Cyclin C-CDK8 (25) (Protein Data Bank accession number 3RGF). Cyclin C, blue; CDK8, gray. Targeted residues that lie within (W177, N181, D182, and Y238) and outside (W6 and E98) the groove are rendered yellow.

(C) Baculovirus-expressed MED12-HA, FLAG-CDK8, and CycC-H6 (WT or mutant as indicated) were immunoprecipitated from infected insect cell lysates. FLAG-specific immunoprecipitates were processed by western blot (WB) using the indicated antibodies (top) or incubated with [γ-^{32}P]-ATP and purified glutathione S-transferase -CTD (bottom). Input (IN) corresponds to 10% of cell lysate used in IP reactions. WBs and kinase reactions were quantified, and binding and kinase levels calculated as described in the legend to Figure 1F. Data represent the average ± SEM of three independent experiments. Asterisks denote statistically significant differences versus WT (Student's t test, $^{**}p < 0.01$, $^{***}p < 0.001$).

(D) FLAG-tagged WT Cyclin C or its indicated mutant derivatives were immunoprecipitated from transfected HEK293 cell lysates. FLAG-specific immunoprecipitates were processed by WB using the indicated antibodies (top) or subjected to in vitro kinase assay as in (C). INPUT corresponds to 10% of cell lysate used in IP reactions. ^{32}P-GST-CTD levels were quantified and expressed relative to the level in the WT Cyclin C IP.

See also Figures S2 and S3 and Table S3.

Our findings that oncogenic exon 2 mutations in *MED12* uncouple Cyclin C-CDK8/19 from core Mediator implicate aberrant CDK8/19 activity in uterine leiomyomagenesis and suggest potential new targets for therapeutic intervention in a tumor type that negatively impacts hundreds of millions of women worldwide. Because CDK8 and CDK19 are both expressed in normal myometrium (and leiomyomas), it is not presently clear to what extent the oncogenic potential of MED12 mutations derive from disruption of Mediator-associated CDK8 versus CDK19 activity. Further studies will be necessary to address this important issue. Our findings further clarify the network of molecular interactions required for Mediator kinase activity and identify the MED12/Cyclin C interface as a prospective therapeutic target in CDK8-driven cancers.

EXPERIMENTAL PROCEDURES

Cloning and Mutagenesis for the MED12 Flp-In 293 T-REx Cells

Site-directed mutagenesis of MED12 to generate the G44D mutant was performed using the primers listed in Table S3. After mutagenesis, the cDNA constructs were cloned into gateway compatible entry vector and finally to pTO_HA_StrepIII_c_GW_FRT destination vector (Varjosalo et al., 2013).

Affinity Purification

For each individual pull-down, a cell pellet derived from 5 × 15 cm dishes (approximately 5 × 10^7 cells) was lysed for 10 min on ice in 5 ml HNN lysis buffer (50 mM HEPES [pH 8.0], 150 mM NaCl, 5 mM EDTA, 0.5% NP-40, 50 mM NaF, 1.5 mM Na3VO4, 1.0 mM phenylmethanesulfonylfluoride, and 10 μl/ml protease inhibitor cocktail [Sigma]). Insoluble material was removed by centrifugation at 13,000 rpm for 20 min at 4°C. A total of 200 μl Strep-Tactin Sepharose beads (400 μl slurry) was transferred to a Bio-Spin chromatography column (Bio-Rad) and washed with 3 × 1 ml HNN buffer and 3 × 1 ml HNN buffer without detergent and inhibitors, and bound proteins were eluted with 3 × 300 μl freshly prepared 0.5 mM D-biotin (Thermo Scientific) in HNN buffer into a fresh 1.5 ml Eppendorf tube.

Mass Spectrometry

Samples were prepared for liquid chromatography MS as follows: dithiothreitol was added to the eluates to a final concentration of 10 mM, and the samples were incubated for 1 hr at 56°C. To block cysteine residues, iodoacetamide was added to a final concentration of 55 mM and the samples incubated at room temperature in the dark for 30 min. A total of 1 μg trypsin was added, and the samples were incubated overnight at 37°C. Tryptic digests were quenched with 10% trifluoroacetic acid (TFA), concentrated and purified by reverse-phase chromatography MicroSpin Column (C18, Nest Group) and eluted with 90% CH3CN, 0.1% TFA. The volume of the eluted sample was reduced to approximately 2 μl in a vacuum centrifuge and reconstituted to a final volume of 40 μl with 0.1% TFA, 1% CH3CN and vortexed thoroughly. Mass spectrometry analysis was performed on an Orbitrap Elite ETD mass spectrometer (Thermo Scientific) using the Xcalibur version 2.7.1 coupled to a Thermo Scientific nLCII nanoflow system (Thermo Scientific) via a nanoelectrospray ion source. Solvents for liquid chromatography MS separation of the digested samples were as follows: solvent A consisted of 0.1% formic acid in water (98%) and acetonitrile (2%), and solvent B consisted of 0.1% formic acid in acetonitrile (98%) and water (2%). From a thermostatted microautosampler, 8 μl of the tryptic peptide mixture (corresponding to 20% of the final eluate) was automatically loaded onto a 15 cm fused silica analytical column with an inner diameter of 75 μm packed with C18 reversed-phase material (Thermo Scientific), and the peptides were eluted from the analytical column with a 40 min gradient ranging from 5% to 35% solvent B, followed by a 10 min gradient from 35% to 80% solvent B at a constant flow rate of 300 nl/min. The analyses were performed in a data-dependent acquisition mode using a top 10 collision-induced dissociation (CID) method. Dynamic exclusion for selected ions was 30 s. No lock masses were employed. Maximal ion

accumulation time allowed on the Orbitrap Elite ETD in CID mode was 100 ms for MSn in the Ion Trap and 200 ms in the Fourier transform mass spectrometer (FTMS). Automatic gain control was used to prevent overfilling of the ion traps and was set to 10,000 (CID) in MSn mode for the Ion Trap and 10^6 ions for a full FTMS scan. Intact peptides were detected in the Orbitrap at 60,000 resolution. Peak extraction and subsequent protein identification was achieved using Proteome Discoverer software (Thermo Scientific). Calibrated peak files were searched against the human component of UniProtKB/SwissProt database (http://www.uniprot.org) by a SEQUEST search engine. Error tolerances on the precursor and fragment ions were ±15 ppm and ±0.6 Da, respectively. Database searches were limited to fully tryptic peptides with maximum one missed cleavage, and carbamidomethyl cysteine and methionine oxidation were set as fixed and variable modifications, respectively.

The normalization of protein abundance is described in Table S1.

Kinase Assays

For in vitro kinase assays, insect cell lysates expressing MED12-hemagglutinin (WT or mutants), CDK8-FLAG, and Cyclin C-H6 (WT or mutants) were combined in different combinations and subjected to FLAG IP for 1 hr at 4°C in 200 mM NaCl D buffer. Immune complexes were washed in 200 mM NaCl D buffer and subjected to a kinase assay containing 25 mM Tris (pH 7.5), 20 mM $MgCl_2$, 2.5 mCi [γ-^{32}P]-ATP, and 2 μg of purified glutathione S-transferase (GST)-3X-CTD. Reactions were incubated for 30 min at 30°C, eluted in Laemmli sample buffer, processed by SDS-12% PAGE, stained with Coomassie blue and visualized by phosphorimager analysis. ^{32}P-labeled GST-3X-CTD was quantified using ImageQuant software.

For in vivo-derived kinase assays, HEK293 cells were transfected with pCDNA3.1-3xFLAG Cyclin C (WT or mutant) or 3xFLAG MED12 (WT or mutant) plasmids and nuclear extracts were harvested 48 hr later. Extracts were subjected to FLAG IP in 200 mM D buffer overnight at 4°C. Immune complexes were washed and subjected to a kinase assay containing 25 mM Tris (pH 7.5), 20 mM $MgCl_2$, 2.5 mCi [γ-^{32}P]-ATP, and 2 μg of purified GST-3X-CTD. Reactions were incubated for 30 min at 30°C, eluted in Laemmli sample buffer, processed by SDS-12% PAGE, stained with Coomassie stain, and visualized by phosphorimager analysis. ^{32}P-labeled GST-3X-CTD levels were quantified using ImageQuant software.

SUPPLEMENTAL INFORMATION

Supplemental Information includes Supplemental Experimental Procedures, three figures, and three tables and can be found with this article online at http://dx.doi.org/10.1016/j.celrep.2014.03.047.

AUTHOR CONTRIBUTIONS

M.T., J.M.S., and M.V. designed and performed research, analyzed data, and wrote the paper; A.V. designed and performed research and analyzed data; S.K., M.J.P., A.D.C., N.M., F.G., H.N., M.A., K.K., and P.V. performed research and analyzed data; T.K., K.P., and C.A.K. analyzed data; and L.A.A., J.T., and T.G.B. designed research, analyzed data, and wrote the paper.

ACKNOWLEDGMENTS

We thank Dr. Mikael Björklund for critical review of the manuscript and Hertta Perikangas-Hentunen, Sini Miettinen, and Michael Parker for technical assistance. This work was supported by the Academy of Finland Center of Excellence in Cancer Genetics, Finnish Cancer Organizations, Sigrid Juselius Foundation, Biocenter Finland, and the U.S. Department of Health and Human Services National Institutes of Health grants MH085320 and AR053100 (T.G.B.). K.P. has been funded by the Finnish Cancer Institute. A.D.C. was supported by COSTAR Program NIDCR grant DE014318.

Received: October 18, 2013
Revised: January 23, 2014
Accepted: March 18, 2014
Published: April 17, 2014

REFERENCES

Akoulitchev, S., Chuikov, S., and Reinberg, D. (2000). TFIIH is negatively regulated by cdk8-containing mediator complexes. Nature *407*, 102–106.

Barbieri, C.E., Baca, S.C., Lawrence, M.S., Demichelis, F., Blattner, M., Theurillat, J.P., White, T.A., Stojanov, P., Van Allen, E., Stransky, N., et al. (2012). Exome sequencing identifies recurrent SPOP, FOXA1 and MED12 mutations in prostate cancer. Nat. Genet. *44*, 685–689.

Conaway, R.C., and Conaway, J.W. (2011). Function and regulation of the Mediator complex. Curr. Opin. Genet. Dev. *21*, 225–230.

Ding, N., Zhou, H., Esteve, P.O., Chin, H.G., Kim, S., Xu, X., Joseph, S.M., Friez, M.J., Schwartz, C.E., Pradhan, S., and Boyer, T.G. (2008). Mediator links epigenetic silencing of neuronal gene expression with x-linked mental retardation. Mol. Cell *31*, 347–359.

Donner, A.J., Ebmeier, C.C., Taatjes, D.J., and Espinosa, J.M. (2010). CDK8 is a positive regulator of transcriptional elongation within the serum response network. Nat. Struct. Mol. Biol. *17*, 194–201.

Firestein, R., Bass, A.J., Kim, S.Y., Dunn, I.F., Silver, S.J., Guney, I., Freed, E., Ligon, A.H., Vena, N., Ogino, S., et al. (2008). CDK8 is a colorectal cancer oncogene that regulates beta-catenin activity. Nature *455*, 547–551.

Glatter, T., Wepf, A., Aebersold, R., and Gstaiger, M. (2009). An integrated workflow for charting the human interaction proteome: insights into the PP2A system. Mol. Syst. Biol. *5*, 237.

Hoeppner, S., Baumli, S., and Cramer, P. (2005). Structure of the mediator subunit cyclin C and its implications for CDK8 function. J. Mol. Biol. *350*, 833–842.

Je, E.M., Kim, M.R., Min, K.O., Yoo, N.J., and Lee, S.H. (2012). Mutational analysis of MED12 exon 2 in uterine leiomyoma and other common tumors. Int. J. Cancer *131*, E1044–E1047.

Kämpjärvi, K., Mäkinen, N., Kilpivaara, O., Arola, J., Heinonen, H.R., Böhm, J., Abdel-Wahab, O., Lehtonen, H.J., Pelttari, L.M., Mehine, M., et al. (2012). Somatic MED12 mutations in uterine leiomyosarcoma and colorectal cancer. Br. J. Cancer *107*, 1761–1765.

Kim, S., Xu, X., Hecht, A., and Boyer, T.G. (2006). Mediator is a transducer of Wnt/beta-catenin signaling. J. Biol. Chem. *281*, 14066–14075.

Knuesel, M.T., Meyer, K.D., Bernecky, C., and Taatjes, D.J. (2009a). The human CDK8 subcomplex is a molecular switch that controls Mediator coactivator function. Genes Dev. *23*, 439–451.

Knuesel, M.T., Meyer, K.D., Donner, A.J., Espinosa, J.M., and Taatjes, D.J. (2009b). The human CDK8 subcomplex is a histone kinase that requires Med12 for activity and can function independently of mediator. Mol. Cell. Biol. *29*, 650–661.

Kornberg, R.D. (2005). Mediator and the mechanism of transcriptional activation. Trends Biochem. Sci. *30*, 235–239.

Larivière, L., Seizl, M., and Cramer, P. (2012). A structural perspective on Mediator function. Curr. Opin. Cell Biol. *24*, 305–313.

Mäkinen, N., Mehine, M., Tolvanen, J., Kaasinen, E., Li, Y., Lehtonen, H.J., Gentile, M., Yan, J., Enge, M., Taipale, M., et al. (2011). MED12, the mediator complex subunit 12 gene, is mutated at high frequency in uterine leiomyomas. Science *334*, 252–255.

Malik, S., and Roeder, R.G. (2010). The metazoan Mediator co-activator complex as an integrative hub for transcriptional regulation. Nat. Rev. Genet. *11*, 761–772.

Mehine, M., Kaasinen, E., Mäkinen, N., Katainen, R., Kämpjärvi, K., Pitkänen, E., Heinonen, H.R., Bützow, R., Kilpivaara, O., Kuosmanen, A., et al. (2013). Characterization of uterine leiomyomas by whole-genome sequencing. N. Engl. J. Med. *369*, 43–53.

Morris, E.J., Ji, J.Y., Yang, F., Di Stefano, L., Herr, A., Moon, N.S., Kwon, E.J., Haigis, K.M., Näär, A.M., and Dyson, N.J. (2008). E2F1 represses beta-catenin transcription and is antagonized by both pRB and CDK8. Nature *455*, 552–556.

Schneider, E.V., Böttcher, J., Blaesse, M., Neumann, L., Huber, R., and Maskos, K. (2011). The structure of CDK8/CycC implicates specificity in the

CDK/cyclin family and reveals interaction with a deep pocket binder. J. Mol. Biol. *412*, 251–266.

Spaeth, J.M., Kim, N.H., and Boyer, T.G. (2011). Mediator and human disease. Semin. Cell Dev. Biol. *22*, 776–787.

Stewart, E.A. (2001). Uterine fibroids. Lancet *357*, 293–298.

Taatjes, D.J. (2010). The human Mediator complex: a versatile, genome-wide regulator of transcription. Trends Biochem. Sci. *35*, 315–322.

Tsai, K.L., Sato, S., Tomomori-Sato, C., Conaway, R.C., Conaway, J.W., and Asturias, F.J. (2013). A conserved Mediator-CDK8 kinase module association regulates Mediator-RNA polymerase II interaction. Nat. Struct. Mol. Biol. *20*, 611–619.

van de Peppel, J., Kettelarij, N., van Bakel, H., Kockelkorn, T.T., van Leenen, D., and Holstege, F.C. (2005). Mediator expression profiling epistasis reveals a signal transduction pathway with antagonistic submodules and highly specific downstream targets. Mol. Cell *19*, 511–522.

Varjosalo, M., Keskitalo, S., Van Drogen, A., Nurkkala, H., Vichalkovski, A., Aebersold, R., and Gstaiger, M. (2013). The protein interaction landscape of the human CMGC kinase group. Cell Rep. *3*, 1306–1320.

Vogelstein, B., Papadopoulos, N., Velculescu, V.E., Zhou, S., Diaz, L.A., Jr., and Kinzler, K.W. (2013). Cancer genome landscapes. Science *339*, 1546–1558.

Zhou, H., Kim, S., Ishii, S., and Boyer, T.G. (2006). Mediator modulates Gli3-dependent Sonic hedgehog signaling. Mol. Cell. Biol. *26*, 8667–8682.

Zhou, H., Spaeth, J.M., Kim, N.H., Xu, X., Friez, M.J., Schwartz, C.E., and Boyer, T.G. (2012). MED12 mutations link intellectual disability syndromes with dysregulated GLI3-dependent Sonic Hedgehog signaling. Proc. Natl. Acad. Sci. USA *109*, 19763–19768.